Diffractive Dijets in DIS and Photoproduction

Matthias U. Mozer
on behalf of the
H1 Collaboration

Physikalisches Institut, Universität Heidelberg, Philosophenweg 12, 69120 Heidelberg, Germany

Abstract. The factorization of diffractive ep cross sections into a (perturbatively accessible) matrix element and a diffractive structure function was proven for the case of DIS by Collins in 1998. This factorization is not expected to hold for Photoproduction. Diffractive dijet production provides a valuable probe to testing factorization and characterize possible mechanisms of factorization breaking. Measurements of dijet cross-sections in DIS and photoproduction made with the H1 detector at the HERA accelerator are presented. Diffractive events were identified by a rapidity gap selection. The resulting differential cross sections are compared to QCD calculations in NLO, based on structure functions extracted from inclusive diffraction. The diffractive dijet cross sections in DIS agree well with the QCD predictions, supporting the QCD factorization for DIS. This is not the case for the diffractive dijet cross sections in photoproduction, which are significantly suppressed with respect to the expectations from QCD factorization.

Keywords: diffraction, factorization
PACS: 12.38.Bx, 12.38.Qk, 12.39.St, 12.40.Nn, 13.87.-a

INTRODUCTION

It can be shown [1] in Quantum Chromodynamics (QCD) that the cross section for diffractive deep-inelastic ep scattering (DIS) factorises into universal diffractive parton densities of the proton and process-dependent hard scattering cross sections (QCD factorisation). Diffractive parton densities have been determined from QCD fits to inclusive diffractive corss sections [2, 3].

Previous measurements of diffractive dijet and D^* meson production in DIS have been found to be described by leading order (LO) Monte Carlo QCD calculations including parton showers (PS) based on diffractive parton densities [5, 6]. However, applying this approach in LO QCD calculations to predict diffractive cross sections for dijet production in $p\bar{p}$ collisions at the Tevatron leads to an overestimation of the observed rate by approximately one order of magnitude [7]. This discrepancy has been attributed to the presence of the additional beam hadron remnant in $p\bar{p}$ collisions, which leads to secondary interactions and a breakdown of factorisation. The suppression, often characterised by a 'rapidity gap survival probability,' cannot be calculated perturbatively and has been parameterised in various ways (see for example [8]).

The transition from deep-inelastic scattering to hadron-hadron scattering can be studied at HERA in a comparison of scattering processes in DIS and in photoproduction. Processes in which a real photon participates directly in the hard scattering are expected to be similar to the deep-inelastic scattering of highly virtual photons. By contrast, processes in which the photon is first resolved into partons which then initiate the hard scat-

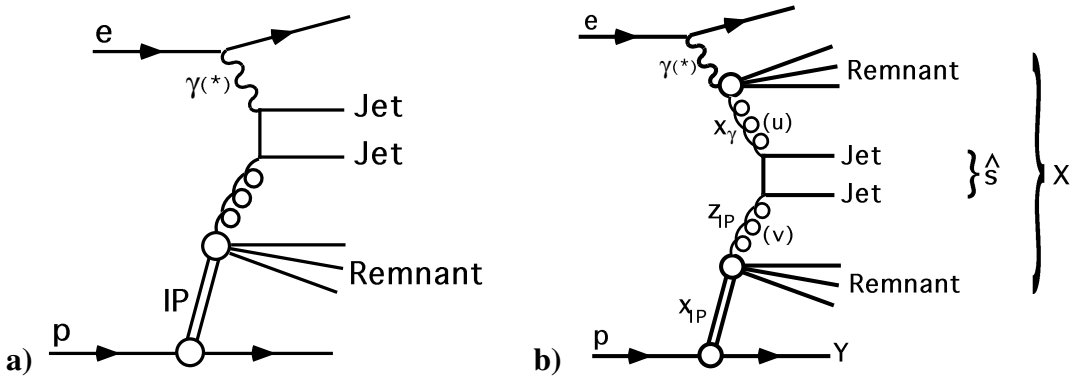

FIGURE 1. Leading order diagrams for diffractive dijet production at HERA. a) Direct (point-like) photon process (photon-gluon fusion), b) resolved (hadron-like) photon process with gluon-gluon scattering. This process can also lead to quark-quark and quark-gluon scattering.

tering resemble hadron-hadron scattering. Via resolved photon processes in hard photoproduction, gluon-gluon and gluon-quark final states are accessible, which are present in the equivalent $p\bar{p}$ collisions but negligible in DIS. Different models for diffractive scattering can therefore be tested in the regime of hard diffractive DIS and photoproduction.

In this article, measurements of diffractive dijet cross sections in DIS and photoproduction are presented, based on data collected with the H1 detector at HERA. Apart from the different range for the photon virtuality, the two measurements are performed in the same kinematic ranges to allow the closest possible comparison of the cross sections. The cross sections are compared with next to leading order (NLO) QCD predictions based on diffractive parton densities.

Examples of hard diffractive processes leading to jets in the final state at HERA are given by the diagrams of Figure 1 for the photon-gluon fusion production mechanism ("direct" photon process) and a process in which the photon develops a hadronic structure from which a single parton undergoes the hard scatter ("resolved" photon process). In photoproduction, resolved processes give a large contribution, whereas in DIS they are suppressed due to the large photon virtuality. The diffractive exchange in these diagrams is modeled by the exchange of the Pomeron with momentum fraction $x_{I\!P}$.

EXPERIMENTAL PROCEDURE

A detailed description of the H1 detector can be found in [9]. The data used in the present analysis were taken in the 1996 and 1997 running periods, in which HERA collided 820 GeV protons with 27.5 GeV positrons, corresponding to an integrated luminosity of 18 pb^{-1}. The photoproduction data are collected using a trigger which requires the scattered positron to be measured in the small angle positron detector, while DIS events are collected using a trigger which requires the scattered positron to be detected in the backward electromagnetic calorimeter. Rapidity gap events are selected by requiring an absence of activity in the direction of the outgoing proton. Jets are formed from the hadronic final state using the inclusive k_T cluster algorithm with a distance parameter of

TABLE 1. The kinematic ranges defining the measured cross sections.

Photoproduction	**DIS**
$Q^2 < 0.01$ GeV^2	$4 < Q^2 < 80$ GeV^2
$165 < W < 242$ GeV	
inclusive k_T jet algorithm, distance parameter=1	
$N_{\rm jet} \geq 2$	
$E_T^{*,\rm jet1} > 5$ GeV	
$E_T^{*,\rm jet2} > 4$ GeV	
$-1 < \eta_{\rm jet(1,2)} < 2$	$-3 < \eta^*_{\rm jet(1,2)} < 0$
$x_{I\!P} < 0.03$	

unity in the γp rest frame. The final jet cross sections are given at the hadron level. The measured distributions are corrected for detector inefficiencies and migrations between measurement intervals during the reconstruction. The kinematic regions in which the cross sections are measured are given in Table 1. The kinematic variables $x_{I\!P}, M_Y$ and t are defined on the basis of the largest rapidity gap in the final state hadron distribution which divides the hadrons into the systems X and Y (the variables are defined as in [5]).

NEXT-TO-LEADING ORDER QCD CALCULATIONS

To calculate diffractive dijet cross sections to NLO in QCD for deep-inelastic positron-proton scattering, the DISENT [10] program is used. To obtain NLO cross sections for diffractive dijet photoproduction, the program by Frixione et al. [11] is used. Both programs are interfaced to the 'H1 2002 fit' (prel.) NLO diffractive parton distributions obtained in [3]. For the comparison with the measured hadron level jet cross sections, the calculated NLO parton jet cross sections were corrected for the effects of hadronisation using the RAPGAP Monte Carlo generator with Lund string fragmentation.

RESULTS

Figure 2 shows the dijet production cross section in diffractive DIS for $z_{I\!P}^{\rm jets}$ (an estimator for the fraction of the momentum of the diffractive exchange entering the hard scatter) and $\log_{10}(x_{I\!P})$ in comparison to the QCD predictions calculated with the DISENT program. Good agreement is found within the given uncertainties for $\log_{10}(x_{I\!P})$. Some discrepancy between data and prediction can be observed for $z_{I\!P}^{\rm jets} > 0.6$. The uncertainty shown in Figure 2 for the NLO prediction does not include the uncertainty of the gluon density as determined from F_2^D which is very large at high $z_{I\!P}$.

The situation is quite different for the dijet production cross sections in diffractive photoproduction (Figure 3). The QCD calculations are higher by a factor ≈ 2 compared with the experimental results. Therefore QCD factorisation seems to be broken in photoproduction.

Figure 4 shows the differential cross section for the diffractive production of two jets in photoproduction as a function of $x_\gamma^{\rm jets}$(the fraction of the photon momentum entering

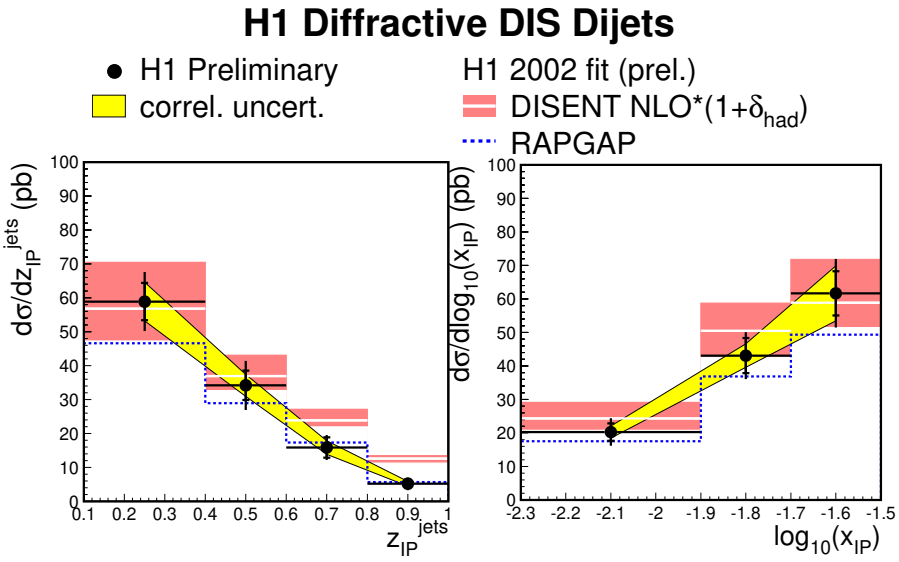

FIGURE 2. Cross section for the diffractive production of two jets in the DIS as a function of a) $z_{I\!P}^{\rm jets}$ and b) $\log_{10}(x_{I\!P})$. The band around the NLO prediction with hadronisation correction indicates the uncertainty resulting from the variation of the renormalisation scale by factors 0.5 and 2. Not shown is the uncertainty resulting from the uncertainty on the diffractive parton densities and the uncertainty due to the imperfect knowledge of the hadronisation corrections.

the hard scatter, $x_\gamma^{\rm jets} = \frac{\Sigma_{\rm jets}(E-p_z)}{2yE_e}$), where the QCD prediction has been modified by two different weighting schemes. In Figure 4 a) the "resolved" part for which $x_\gamma^{\rm jets} < 0.9$ at the parton level is scaled by a factor 0.34 as proposed by Kaidalov et al. [8]. The calculation for $x_\gamma^{\rm jets} > 0.9$ is left unscaled.

In Figure 4 b) the whole QCD calculation was globally scaled down by a factor 0.5. The global scaling of the QCD prediction describes the differential cross section much better than the QCD prediction weighted according to Kaidalov et al. [8].

The global suppression of the QCD calculation by a factor 2 yields a good description of all measured cross sections (see also Figure 5) and is favored over the suppression of only the resolved contribution.

SUMMARY

QCD factorisation in diffraction is tested with diffractive dijet production at HERA. While in the DIS case the measurement supports factorisation, the calculation in photoproduction has to be suppressed by a global factor 2.

REFERENCES

1. J. Collins, *Phys. Rev.* **D 57** (1998) 3051 and erratum ibid. **D61** (2000) 019902.
2. H1 Collaboration, C. Adloff *et al.*, *Z. Phys.* **C 76** (1997) 613.

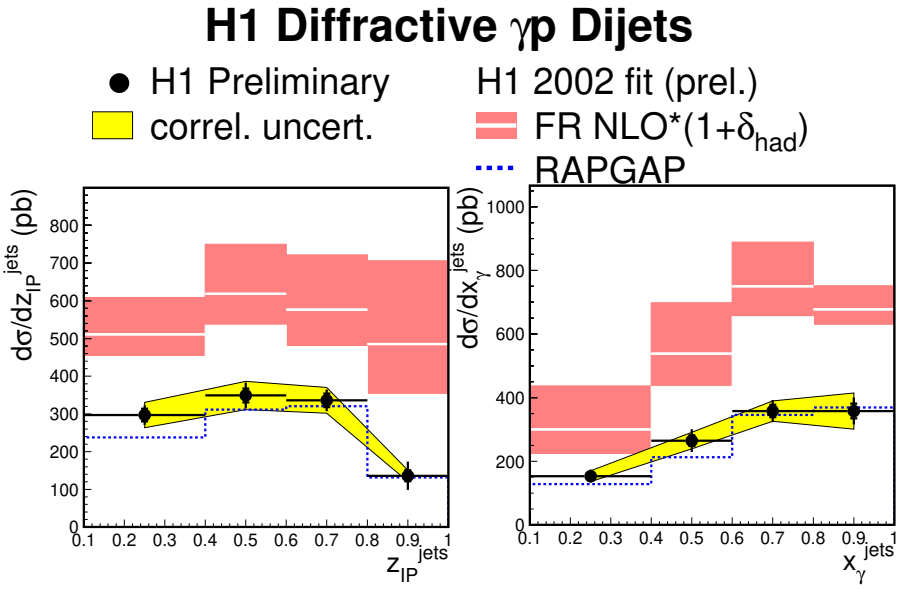

FIGURE 3. Cross section for the diffractive production of two jets in photoproduction as a function of a) $z_{I\!P}^{\rm jets}$ and b) $x_\gamma^{\rm jets}$.The band around the NLO prediction with hadronisation correction indicates the uncertainty resulting from the variation of the renormalisation scale by factors 0.5 and 2.

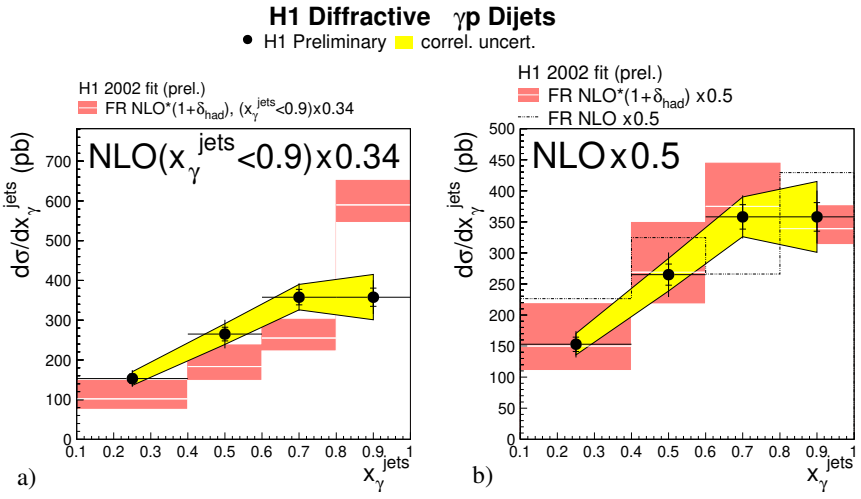

FIGURE 4. Cross section for the diffractive production of two jets in photoproduction as a function of $x_\gamma^{\rm jets}$. In a) the resolved contributions to the QCD calculation ($x_\gamma^{\rm jets} < 0.9$) is multiplied by 0.34 as proposed by Kaidalov et al. [8], while in b) the complete prediction is multiplied by a factor 0.5.

3. H1 Collaboration, paper 980 submitted to 31st Intl. Conf. on High Energy Physics, ICHEP 2002, Amsterdam.
4. H1 Collaboration, C. Adloff *et al.*, *Eur. Phys. J.* **C 6** (1999) 421.
5. H1 Collaboration, C. Adloff *et al.*, *Eur. Phys. J.* **C 20** (2001) 29.
6. H1 Collaboration, C. Adloff *et al.*, *Phys. Lett.* **B 520** (2001) 191.
7. CDF Collaboration, T. Affolder *et al.*, *Phys. Rev. Lett.* **84** (2000) 5043.

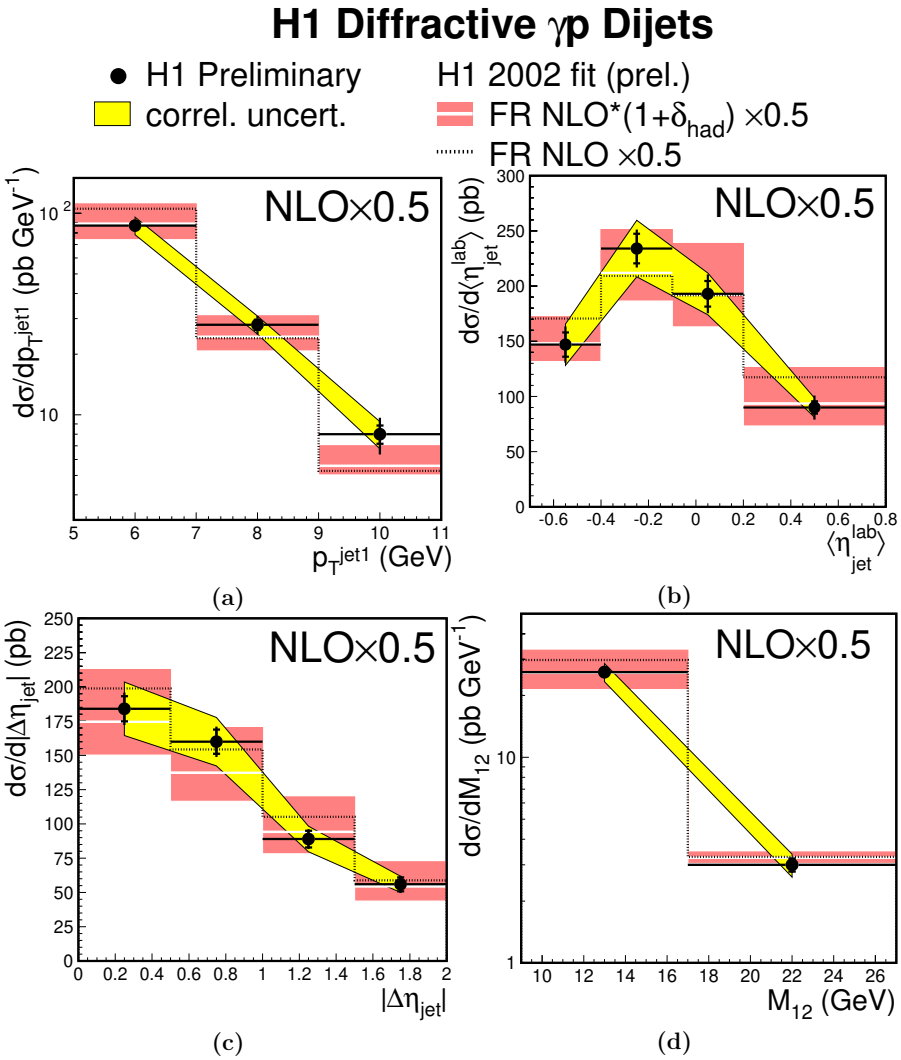

FIGURE 5. Cross section for the diffractive production of two jets in photoproduction as a function of a) p_T^{jet1}, b) $\langle \eta_{\mathrm{jet}}^{\mathrm{lab}} \rangle$, c) $\left|\Delta\eta_{\mathrm{jet}}\right|$ and d) M_{12}.

8. A. Kaidalov, V. Khoze, A. Martin, M. Ryskin, *Phys. Lett.* **B 567** (2003) 61
9. H1 Collaboration, I. Abt *et al.*, *Nucl. Instrum. Methods* **A 386** (1997) 310 and 348.
10. S. Catani, M. H. Seymour, *Nucl. Phys.* **B 485** (1997) 29 [erratum ibid. **B510** (1997) 503].
11. S. Frixione, Z. Kunszt and A. Signer, *Nucl. Phys.* **B 467** (1996) 399;
    S. Frixione, *Nucl. Phys.* **B 507** (1997) 295.